ASIA-PACIFIC
SOLAR RESEARCH
CONFERENCE

Mehrdad Khamooshi

The Effect of Wind on the Performance of the Three Short Natural Draft Dry Cooling Towers in an In-line Arrangement

Mehrdad Khamooshi[1], Timothy Anderson[1], and Roy Nates[1]

[1]Department of Mechanical Engineering, Auckland University of Technology, Auckland, New Zealand
E-mail:timothy.anderson@aut.ac.nz

Abstract

Natural draft dry cooling tower (NDDCT) are a favourable choice for the cooling system of concentrated solar thermal power (CSP) plants located in arid regions with high solar radiation. However, additional cooling towers may be required as the capacity of the CSP plants is increased. The geometrical arrangement of the NDDCTs is an influencing parameter on the thermo-flow performance of the entire system. The aim of this study was to investigate the effect of tower spacing and crosswind velocity on the performance of three short NDDCTs in an in-line layout. The results showed that there is a noticeable interaction between the towers at different tower spacings and crosswind conditions. In the no-wind condition, the cooling performance of both towers is reduced with a small tower-spacing, as this limits the air supply and the airflow across the heat exchangers in both towers. However, in windy conditions, the redirection of flow due to the layout of the cooling towers can improve the performance of the towers. The performance of the middle and leeward tower is improved compared to the windward tower. This improvement becomes weaker with increasing tower spacing.

1. Introduction

The thermo-flow performance of a single short NDDCT has been the subject of numerous studies (Li et al., 2015; Li et al., 2018; Li et al., 2017b; Li et al., 2017c; Lu et al., 2015; Lu et al., 2013; Lu et al., 2014; Lu et al., 2018). However, there is a significant lack of research into the performance of the multiple NDDCTs. The significance of this oversight becomes apparent when considering the potential expansion of a CSP plant; as the capacity of CSP plants is increased, additional cooling is required which necessitates the addition of more NDDCTs. This, in turn, raises the question of where additional towers should be positioned such that cooling performance of the group is maximised, or at least not reduced.

Very few studies have examined the performance of multiple cooling towers in close proximity, and those that have been undertaken investigated the performance of large NDDCTs under windy conditions (Wu and Koh, 1977; Zhai and Fu, 2006). No study has investigated the airflow characteristics around three short NDDCTs during windy conditions was not discussed in any detail. In light of this, this study set out to investigate the effect of wind on three NDDCTs arranged in line, parallel to the prevailing wind direction, at various equal tower spacings.

2. Method

For this study a cylindrical tower and horizontally-arranged air-cooled heat exchanger were examined. As a benchmark, it was decided to investigate the airflow characteristics around a single NDDCT and compare the results to data available in the literature. To achieve this a series of steady-flow, three-dimensional CFD simulations was undertaken using a commercial finite volume solver. A computational domain as shown in Figure 1 was used and dimensions of the computational domain were selected based on a mesh sensitivity analysis that showed the boundaries did not affect

the domain flow field. This resulted in the simulation domain having a height of 90 m, a breadth of 144 m, and a length of 150 m, consisting of over 3.2 million structured elements while the element size of the tower and heat exchanger was set to 0.25

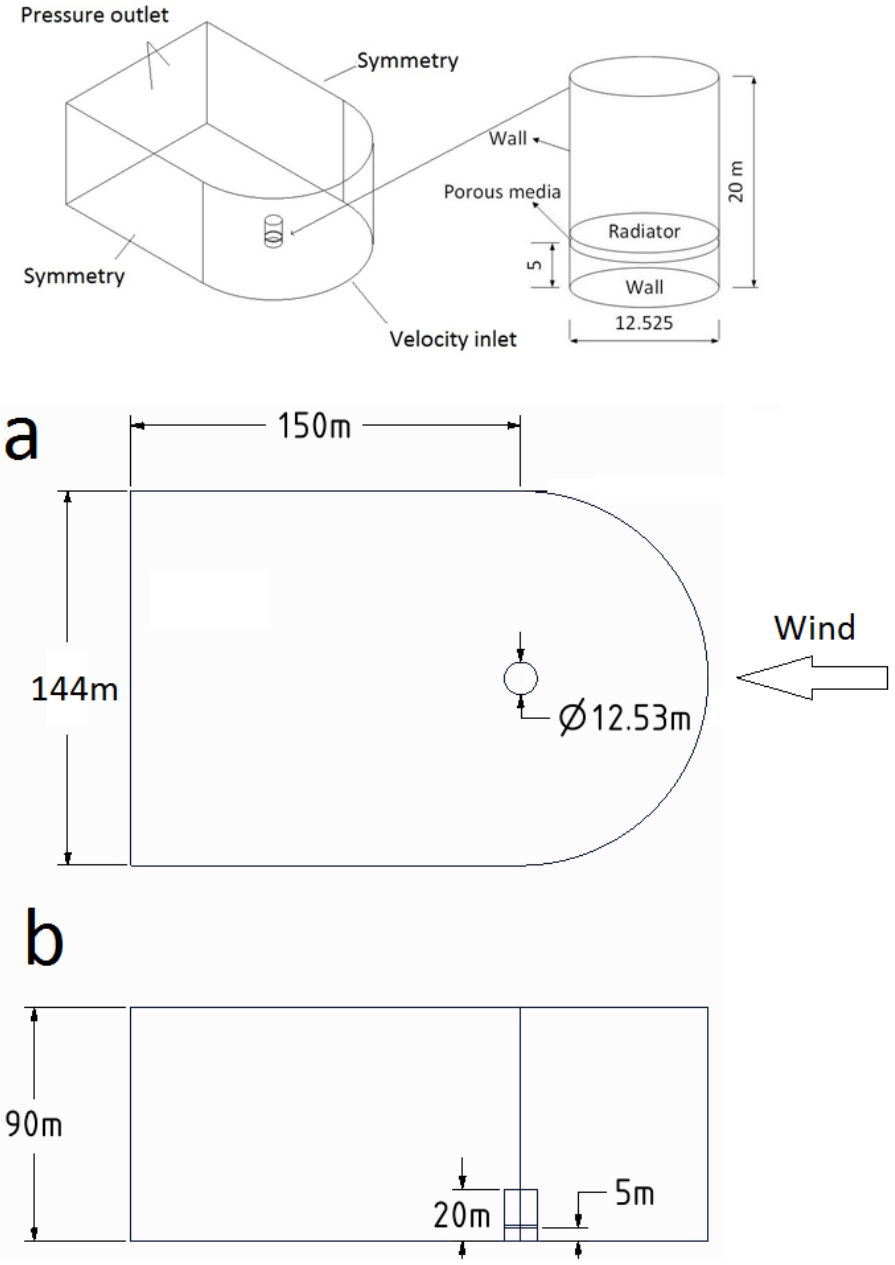

Figure 1. Computational domain and boundary conditions at a) plan view b) side elevation

In order to model the heat exchanger in the tower, a combination of a porous media zone and a radiator boundary condition was used. This approach had previously been successfully used for heat exchanger modelling in short NDDCTs (Li et al., 2016; Li et al., 2017c; Lu et al., 2013; Lu et al., 2014). The radiator model characterizes the heat transfer, while the porous media is included to capture the pressure loss within the heat exchanger. This effect is realised by adding a momentum

sink in the governing momentum equations, where the heat exchanger parameters were taken from (Li et al., 2016).

Following on from this, the heat rejected to the surrounding air was given by Equation 1.

$$q = h(T_r - T_{ao}) \quad (1)$$

Furthermore, the heat transfer coefficient and the pressure drop were specified as equations 2 and 3.

$$h = \sum_{n-1}^{3} h_n \, v^{n-1} \quad (2)$$

$$S_i = -(\frac{\mu}{\alpha} v_i + C_2 \frac{1}{2} \rho |v| v_j) \quad (3)$$

Where 1/α is the viscous resistance factor and C2 is the inertial resistance factor.

The values for viscous resistance factor, interial resistance, and heat transfer coefficients are listed in (Li et al., 2017b; Lu et al., 2018) based on the data provided by heat exchanger manufacturer.

In this study, the heat-exchanger parameters were identical to those of Li et al. (Li et al., 2016) and the geometric parameters were made as similar to this study as possible.

For windy conditions, a velocity inlet boundary condition was assigned at the windward side of the domain, where the velocity profile applied was defined by equation 4 (Li et al., 2015; Lu et al., 2014):

$$U = v_{cw} = (\frac{y}{y_{ref}})^a v_{ref} \quad (4)$$

where v_{ref} is a reference velocity at a reference height, y_{ref}=10 m, and exponent a is defined as the roughness of the ground and the stability of the atmosphere, taken to be 0.2 (Yang et al., 2011). The values of the turbulent intensity (0.1%) and viscosity ratio (0.1) were taken from the (Li et al., 2015; Zhao et al., 2015) due to low-turbulence level of advection natural wind. The pressure outlet was assigned to the outlet and top surfaces of the domain where the static pressure was assumed as zero. A constant ambient temperature of 20 °C was assumed.

The turbulent field was simulated using the realizable k-ε turbulence model. Realizbale k-ε has been extensively validated for a wide range of flows including rotating shear flows, boundary layer flows and separated flows and had been shown to be well suited to modelling both short and large NDDCTs (Lu et al., 2013; Wu et al., 2014). The governing equations can be expressed as general form :

$$\nabla . (\rho u \emptyset - \Gamma_\emptyset \nabla_\emptyset) = S_\emptyset \quad (5)$$

the expression of the $\emptyset$, $\Gamma_\emptyset, and \ S_\emptyset$ in the above equation are listed in Table 1.

Table 1. The governing equations of k- ε model.

	$\emptyset$	$S_\emptyset$	$\Gamma_\emptyset$
Continuity	1	0	0
x momentum	U	$-\frac{\partial p}{\partial x} + \frac{\partial}{\partial x}\left(\mu_e \frac{\partial U}{\partial x}\right) + \frac{\partial}{\partial y}\left(\mu_e \frac{\partial V}{\partial x}\right) + \frac{\partial}{\partial z}\left(\mu_e \frac{\partial W}{\partial x}\right) + \frac{\Delta p_x A_c}{V_c}$	μ_e
y momentum	V	$-\frac{\partial p}{\partial y} + \frac{\partial}{\partial x}\left(\mu_e \frac{\partial U}{\partial y}\right) + \frac{\partial}{\partial y}\left(\mu_e \frac{\partial V}{\partial y}\right) + \frac{\partial}{\partial z}\left(\mu_e \frac{\partial W}{\partial y}\right) + \frac{\Delta p_y A_c}{V_c}$	μ_e
z momentum	W	$-\frac{\partial p}{\partial z} + \frac{\partial}{\partial x}\left(\mu_e \frac{\partial U}{\partial z}\right) + \frac{\partial}{\partial y}\left(\mu_e \frac{\partial V}{\partial z}\right) + \frac{\partial}{\partial z}\left(\mu_e \frac{\partial W}{\partial z}\right) + \frac{\Delta p_z A_c}{V_c}$	μ_e

Energy	T	$\frac{1}{C_p}(\frac{qA_c}{V_c})$	$\frac{\mu}{Pr}+\frac{\mu_t}{Pr_t}$
Turbulent energy	k	$G_k+G_b-\rho\varepsilon$	$\frac{\mu_e}{\sigma_k}$
Energy dissipation	ε	$C_{1\varepsilon}\frac{\varepsilon}{k}(G_k+C_{3\varepsilon}G_b)-C_{2\varepsilon}\rho\frac{\varepsilon^2}{k}$	$\frac{\mu_e}{\sigma_k}$

Where

$$G_k=\mu_e\{2\left[\left(\frac{\partial V}{\partial x}\right)^2+\left(\frac{\partial V}{\partial y}\right)^2+\left(\frac{\partial V}{\partial z}\right)^2\right]+\left(\frac{\partial V}{\partial x}+\frac{\partial U}{\partial y}\right)^2+\left(\frac{\partial V}{\partial z}+\frac{\partial W}{\partial y}\right)^2+$$

$$\mu_e=\mu+\mu_t;\ \mu_t=C_\mu\rho\frac{k^2}{\varepsilon};\ \ C_{1\varepsilon}=1.44;\ C_{2\varepsilon}=1.92;\ C_{3\varepsilon}=\tanh\left(\frac{U_{pa}}{U_{pe}}\right);\ G_g=-g\frac{U_t}{\rho Pr}\frac{\partial P}{\partial y};\ C_\mu=0.09;\ \sigma_k=1.0;\ \sigma_{k\varepsilon}=1.3;\ Pr=0.74;\ Pr_t=0.85$$

SIMPLEIC (pressure-based segregated algorithms) was applied and the governing equations were discritized using second order of upwind method.

The performance of the simulated cooling tower in windy conditions was compared with previous published works (Li et al., 2015). On this basis, simulations of single NDDCTs were performed at various wind velocities (0-8 m/s). shows a comparison of the normalised heat rejection ($Q/Q_{no\text{-}wind}$) of a single cooling tower for windy conditions between this study and those of Li et al. (Li et al., 2015). The comparisons indicate that the results of both this and the previous study follow the same trend, and the magnitude of the results is broadly similar (less than 5% difference), thus implying a validation of the simulated results from this study.

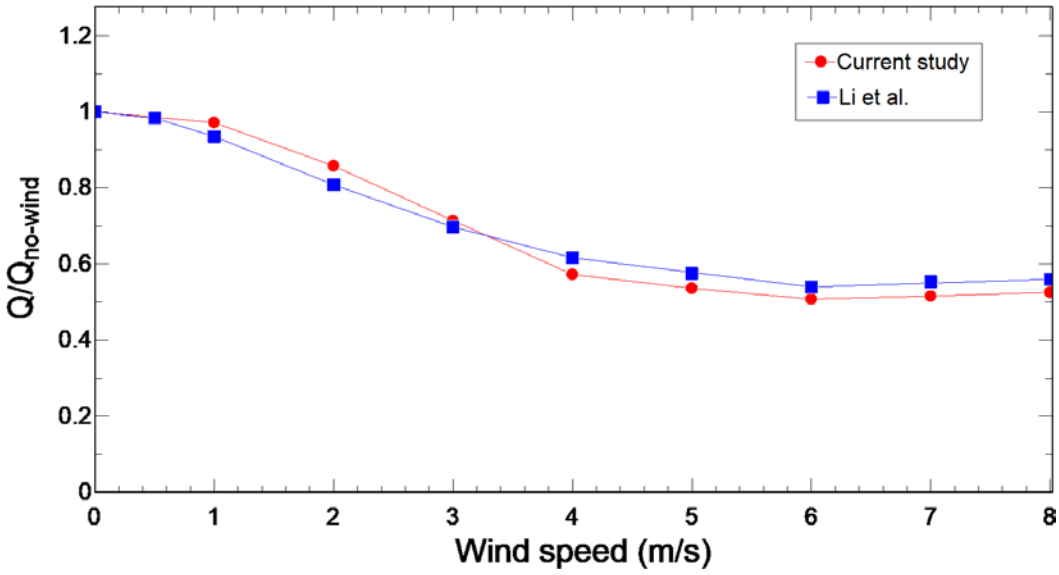

Figure 2. Comparison between the CFD result and previous studies

To further validate the accuracy of the applied numerical set, the results of this study are compared with the experimental results from the real NDDCT in University of Queensland (Li et al., 2017a) (Li et al., 2018; Lu et al., 2018). In the experimental tests, a constant heat was supplied to the NDDCT by an oil-fired heater at different ambient temperatures and the air temperature leaving the heat exchanger was measured. In the CFD simulation, the same heat flux (845kW) was set and the effect of changing the ambient temperature on the air exit temperature at heat exchanger was monitored.

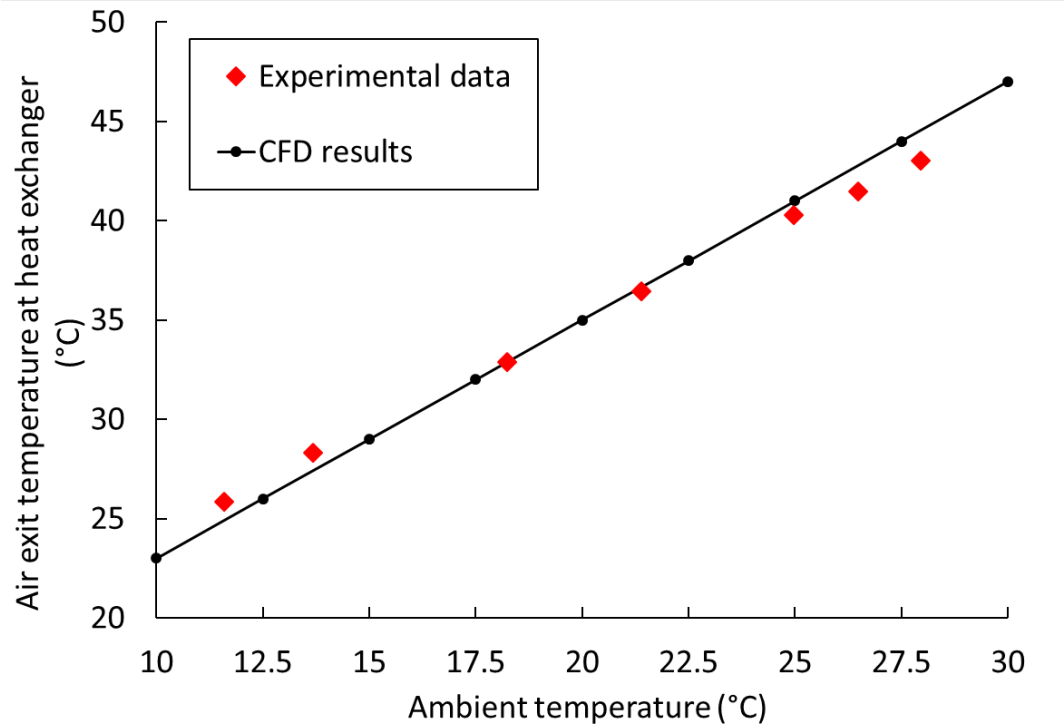

Figure 3. Comparison between the CFD results and the experimental data (Lu et al., 2018).

The same geometry and numerical set as explained in the validation were subsequently used to determine the performance of the three NDDCTs during windy conditions. The cooling towers were placed in a computational domain as shown in Figure 4. The computational domain for three NDDCTs was extended so the outlet boundary does not affect the flow field. The entire computational domain was discretised using 4.6 million structured mesh. A grid-independence test was used, and the results varied by less than 1% when the number of cells was over 4,600,000. To ensure that the model in this study was able to predict the flow field around multiple NDDCTs, the grid generation process was performed carefully, to maximize the quality of the mesh.

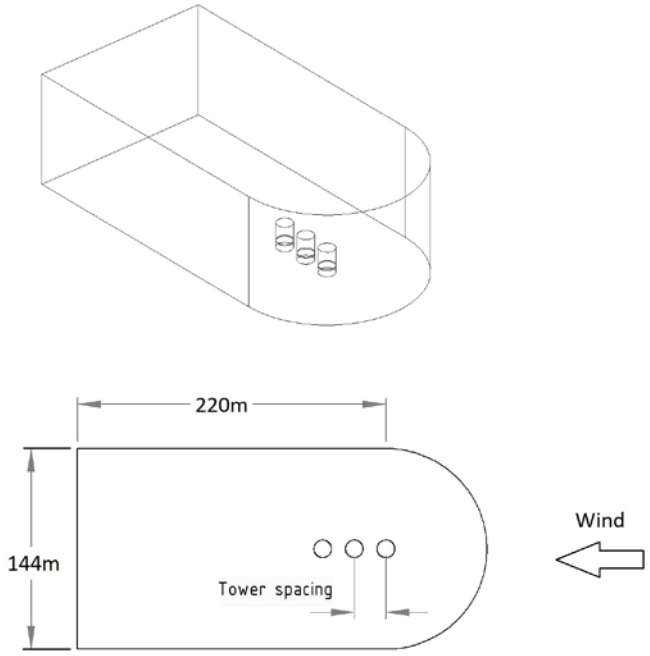

Figure 4. Computational domain and boundary conditions.

3. Results and discussion

The flow and temperature fields of the NDDCTs at various wind velocities and tower spacings were investigated. To observe the relation between the temperature and flow fields on the thermo-flow performance of the towers, the heat rejection of the NDDCTs at different tower spacings and various wind speeds was calculated. In addition, the thermal performance of each tower at different conditions was normalized with respect to the heat rejection rate of an isolated cooling tower under a no-wind condition.

Figure 5 shows the heat rejection of the windward tower at different tower spacings. At v_{cw}=0 m/s, the heat rejection of the windward tower increases by increasing the tower spacing. This is because at low tower-spacings the performance of the towers is exacerbated by the interference of the towers. For the other wind velocities the variation of the tower spacing did not affect the performance of the windward tower, except at v_{cw}=8m/s, where the heat rejection of the windward tower was higher than that of v_{cw}=6 m/s. It should be noted that the heat transfer within a NDDCT occurs by two mechanisms: the heat taken away by the air moving toward the top of the tower (natural convection), and heat taken away by the air that leaves through the bottom part of the tower after circulating around the heat exchangers driven by the lower vortex (force convection). The heat transfer coefficient of a plane's forced convection can be determined using $Nu = aRe_x Pr^{1/3}$, where Re_x is the Reynolds number based on v_{cw} and the length of the heat exchanger (Cengel and Ghajar, 2011; Li et al., 2018). Therefore, the heat transferred by the forced convection is enhanced by with an increase in v_{cw}.

At v_{cw}>6 the radiator's temperature starts to drop which is due to the forced convection at the bottom of the heat exchangers. Increasing the crosswind speed may increase the heat rejection rate of the cooling tower and compensate for a level of thermal efficiency loss in the cooling tower. However, the existence of $v_{cw}$is still an undesirable effect on the thermal performance of the tower since the working mechanism of a cooling tower is based on the natural draft. The point at which the cooling

performance of the heat exchangers starts to increase in the presence of a crosswind is called the "turnaround" point.

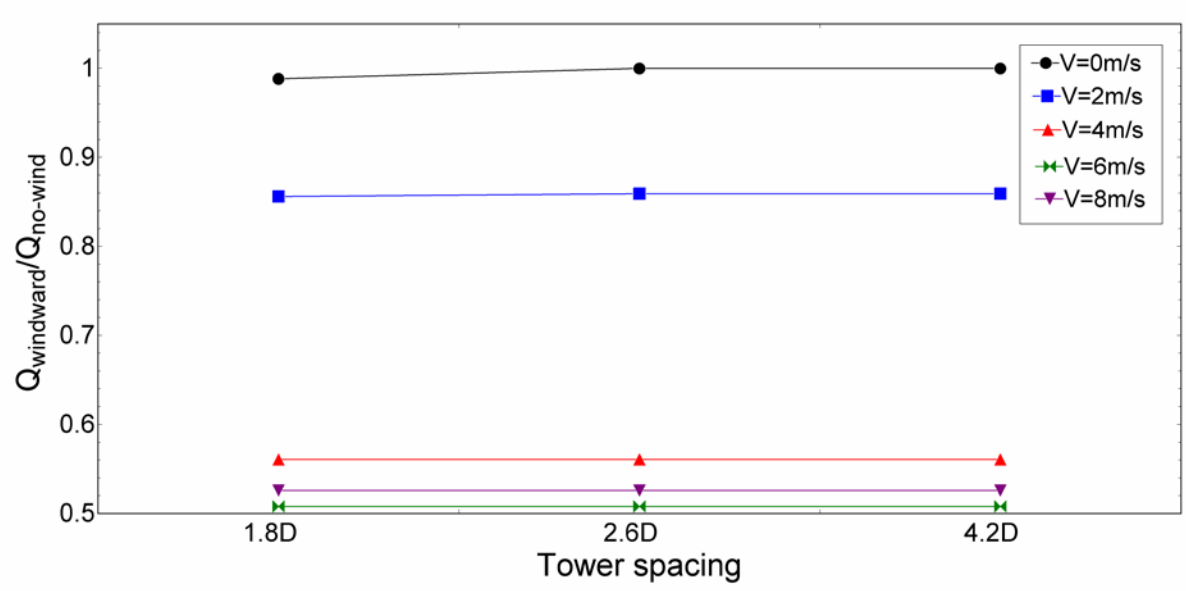

Figure 5. Normalized heat rejection of the windward tower at different tower spacings

Following on from this, the heat rejection rate of the middle tower at different tower spacings is shown in Figure 6. By comparing the heat rejection of the windward and middle towers in a no-wind condition, it can be seen that the middle tower's heat rejection is less than the windward tower's. The middle tower is flanked by two towers and hence the middle tower is interfering with the other two towers in a way that is not beneficial to its performance. At v_{cw}=2m/s, the thermal performance of the middle cooling tower is enhanced at a tower spacing of 2.6D. At a tower spacing of 1.8D, the middle tower continues to interfere with the other two side-towers, which causes flow instabilities within the middle tower and this decreases the heat rejection rate despite the protection provided by the windward tower.

However, at a tower spacing of 4.2D, the intrusion between the towers diminishes and the middle tower benefits from the windward tower's protection. By increasing the tower spacing to 4.2D, there is no confliction for the middle tower and the windward tower continues to protect the middle tower from the upcoming wind. It is clear that this protection is reduced for a large tower-spacing compared to the tower spacing of 2.6D, this results in lower heat rejection for the middle tower at v_{cw}=2m/s. At v_{cw}=4, 6, and 8 m/s, the ambient condition is no longer calm and there is no effect due to the other towers. Overall, it is clear that by increasing the wind speeds, the heat rejection rate of the middle tower decreases.

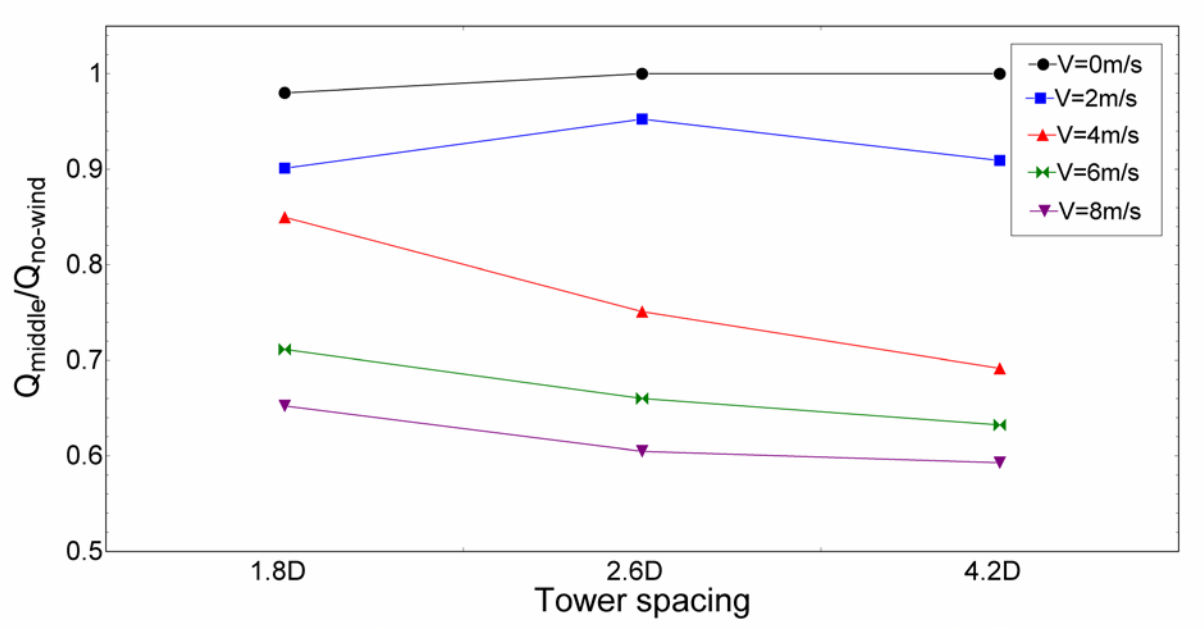

Figure 6. Normalized heat rejection of the middle tower at different tower spacings.

The detailed heat rejection of the leeward tower at various tower spacings is shown in Figure 7. The heat rejection behaviour of the leeward tower is similar to the windward tower in a no-wind condition. At v_{cw}=2m/s, the thermal performance of the tower is enhanced by increasing the tower spacing. This is because, at a low tower-spacing the leeward tower is placed in a zone in which the wake of the windward tower reaches the sides of the leeward tower and causes a flow disturbance for this tower. By increasing the tower spacing, this effect disappears and the leeward tower benefits from the protection provided by the middle and windward towers.

By comparing the heat rejection of the middle tower at a tower spacing of 1.8D ($Q_{middle}/Q_{no\text{-}wind}$=0.77) with the leeward tower ($Q_{middle}/Q_{no\text{-}wind}$=0.69) at v_{cw}=4m/s, it can be seen that the middle tower performs better in such conditions. As explained, the wake of the windward tower at low tower-spacing affects the leeward tower more than the middle tower. However, at this wind speed, low tower-spacing still provides better protection for the leeward tower and the heat rejection rate of the leeward tower decreases by increasing the tower spacing. This is also similar for v_{cw}=6 and 8m/s, which shows that the lower tower-spacing results in better conservation of the upcoming wind for the leeward tower.

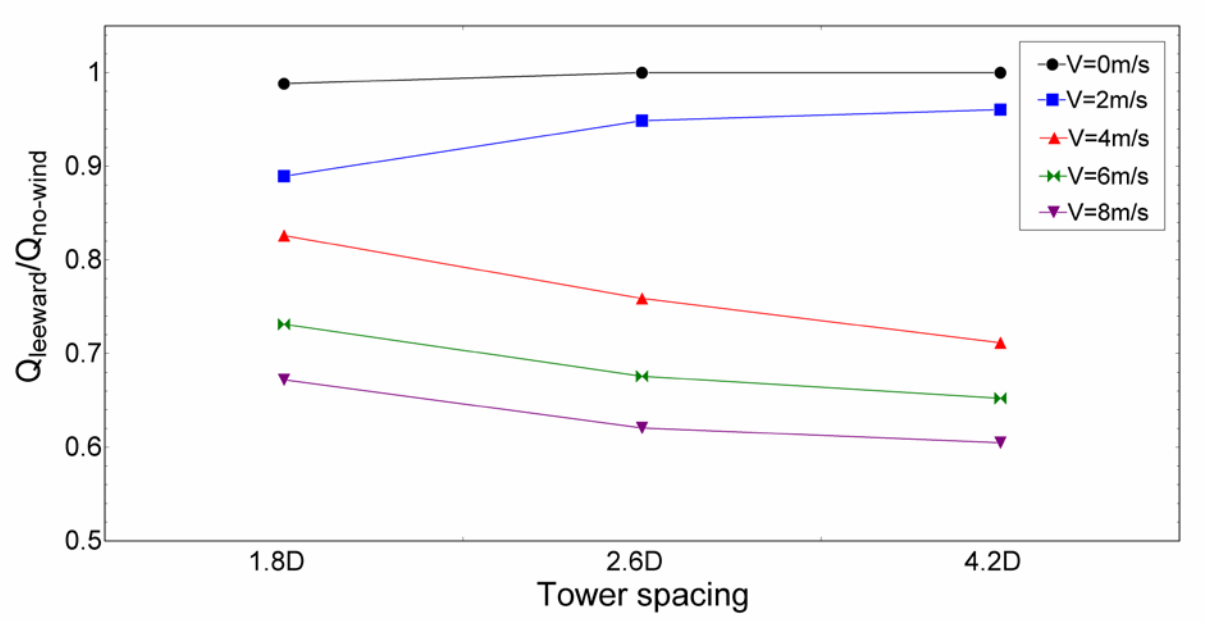

Figure 7. Normalized heat rejection of the leeward tower at different tower spacings.

In Figures, 7-9 the performance of each tower in a multi-tower system is compared with an individual tower. In doing this a metric, δ defined by Equation 5, is introduced to compare the performance of a NDDCT when it is placed in a multi-tower system compared to the same tower on its own.

$$\delta = \frac{Q_{cw} - Q_{Isolated_{cw}}}{Q_{Isolated_{cw}}} * 100 \quad \text{where Crosswind velocity (cw) =0-8 m/s} \qquad (5)$$

Figure 8 shows the performance evaluation of the towers at a tower spacing of 1.8D. For the no-wind condition, the middle tower performs worse than the other towers due to the tower competing with the outer towers for air. The performance change of the windward tower is 0% for windy conditions, which means that the windward tower acts as an isolated cooling tower except in no-wind conditions. At low-wind velocities the performance of the middle tower is reduced (by 7%) compared to an isolated cooling tower. At 2< v_{cw}<6, there is significant protection provided by the windward and leeward towers for the middle tower and its performance is improved about 51% at v_{cw}=5m/s. This can be significantly observed in Figure 9 which shows the velocity streamlines at a height of 5 m at two different crosswind velocities. At v_{cw}=4 m/s the streamlines contact with the leeward tower more than the middle tower, while at v_{cw}=8 m/s, the leeward is the tower which gets more protection from the front tower.

The tower spacing of 1.8D provides a substantial protection for the middle and leeward towers from the upcoming wind (v_{cw}>3).

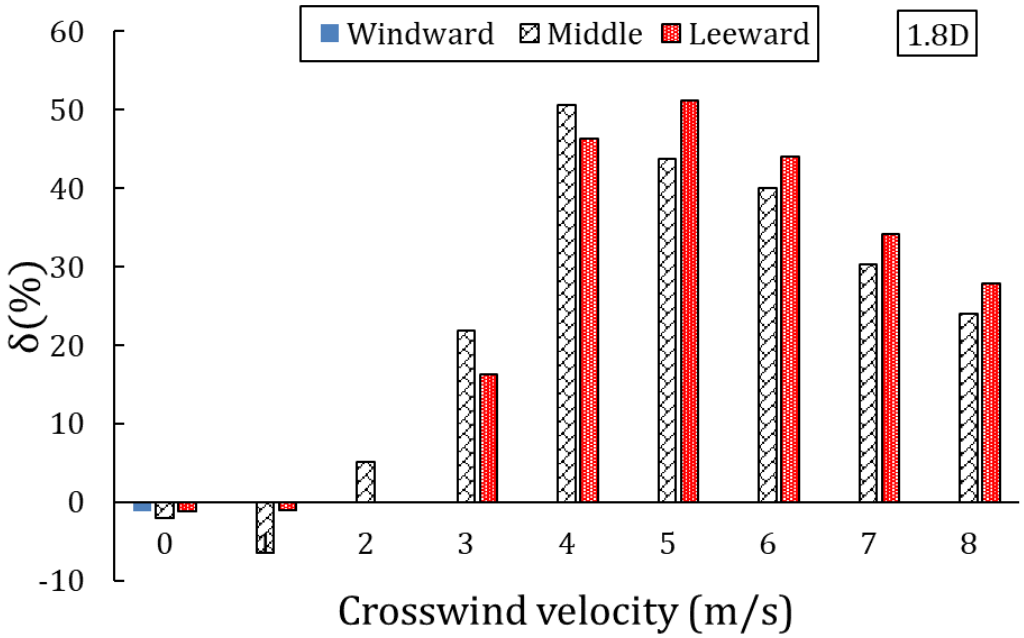

Figure 8. Performance evaluation of the towers at tower spacing of 1.8D.

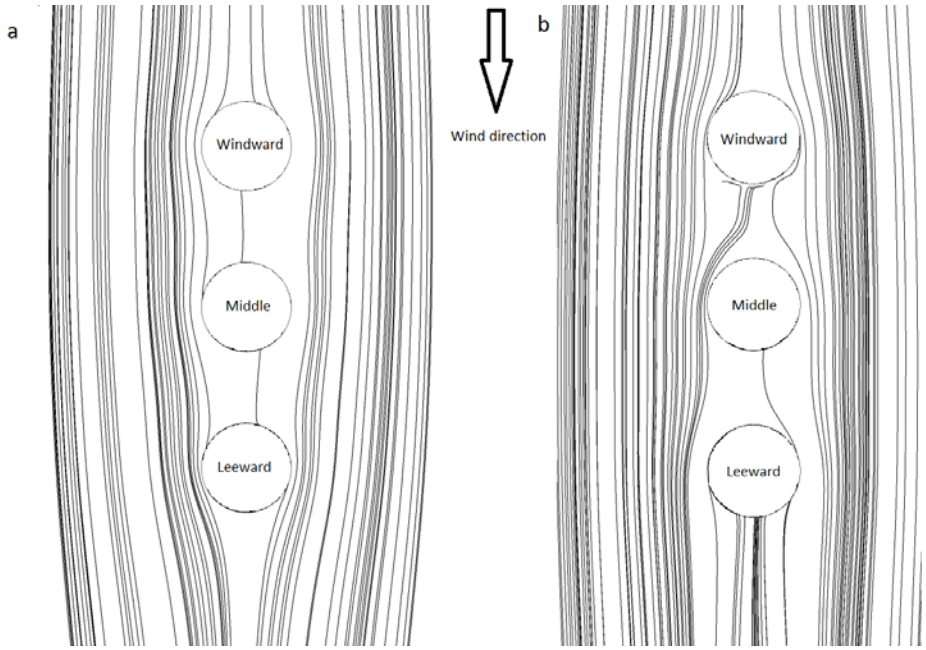

Figure 9. Surface velocity streamlines at height 5m at a) v_{cw}=4 m/s b) v_{cw}=8 m/s at tower spacing of 1.8D

At a tower spacing of 2.8D, the interference between the towers diminishes and in a no-wind condition the towers act as isolated NDDCTs (Figure 10). However, the heat rejection of the middle tower is higher than that of the leeward tower at v_{cw}=1 and 2 m/s. As discussed, the wake passing over the windward tower converges around the leeward tower at low wind speeds which explains

this phenomenon. Further, the performance of the middle and leeward towers is improved for v_{cw}>1 by about 10-33% at this tower spacing. Figure 11 depicts the velocity streamlines at a height of 5 m from the ground, and at v_{cw}=4 m/s the velocity streamlines reaching to the middle and leeward towers are similar. At v_{cw}=8 m/s, the protection of the windward and middle towers is clear and the streamlines which reach to the leeward tower are less than the middle tower.

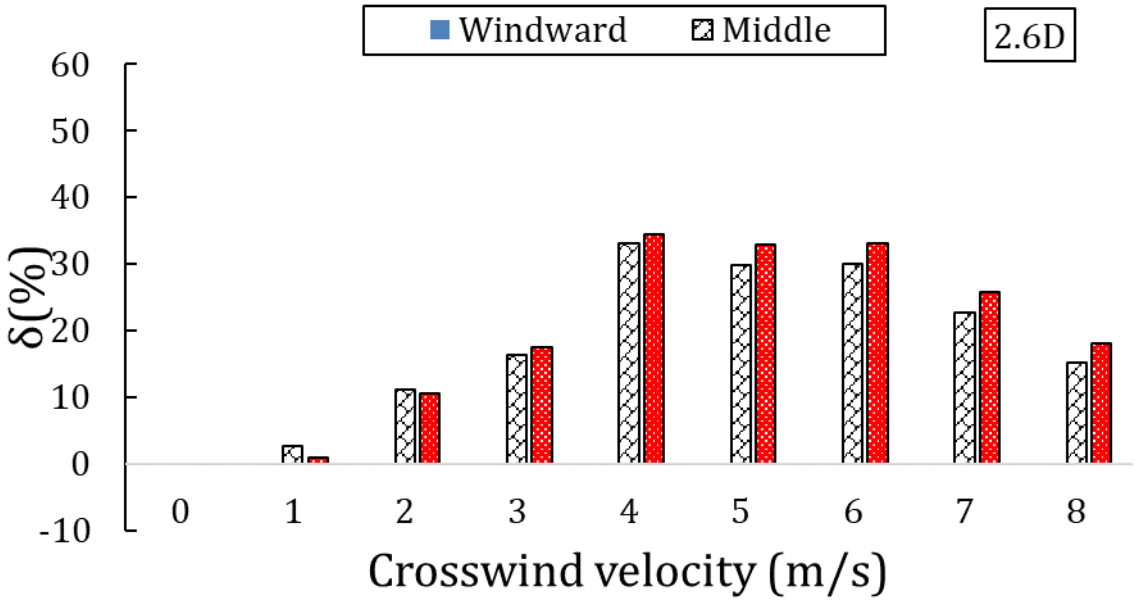

Figure 10. Performance evaluation of the towers at tower spacing of 2.6D.

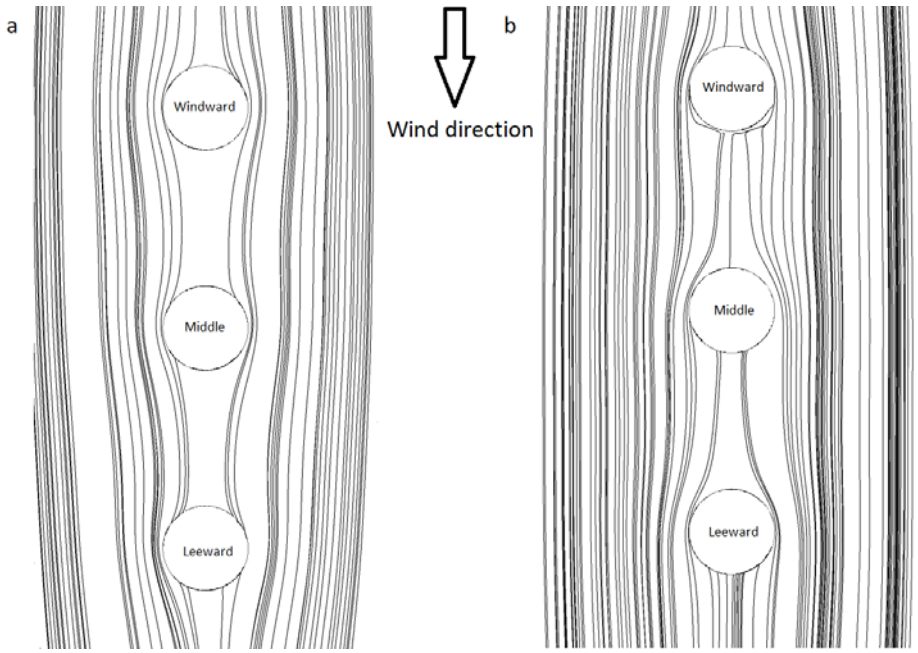

Figure 11. Surface velocity streamlines at height 5m at a) v_{cw}=4 m/s b) v_{cw}=8 m/s at tower spacing 2.6D.

The thermal performance of the towers compared with an isolated cooling tower at tower spacing of 4.2D is presented in Figure 12. Here, the leeward tower benefits from the protection provided by the middle and windward towers, for all wind speeds the leeward tower performs better than the middle tower. Increasing the tower spacing, the protection from the windward tower decreases for the rear towers. Therefore, the performance improvement of the middle and leeward towers at a tower spacing of 4.2D is less than that at 1.8D.

Figure 13 demonstrates the velocity streamlines at a height of 5 m at a tower spacing of 4.2D. At both v_{cw}= 4m/s and 8m/s the crosswind reaches the leeward tower more than the middle tower. By increasing the wind velocity this protection from the wind attack to the leeward tower provided by the middle tower becomes more significant.

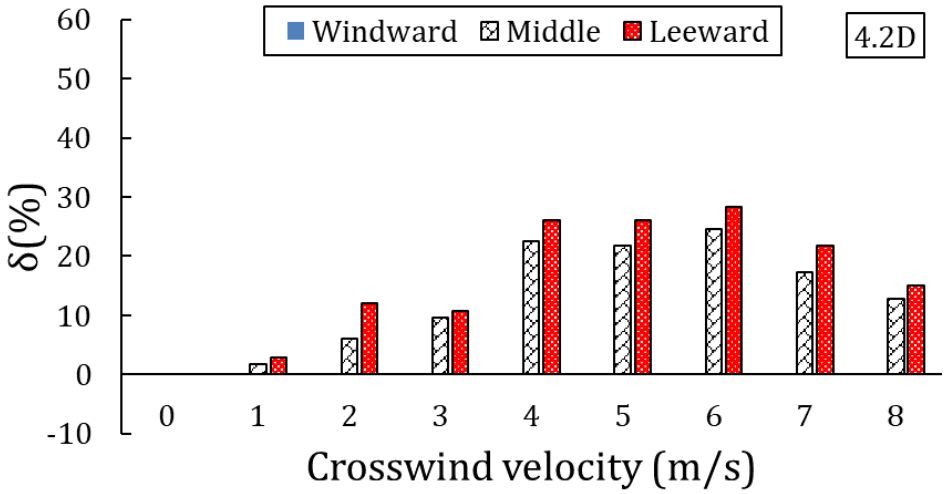

Figure 12. Performance evaluation of the towers at tower spacing of 4.2D.

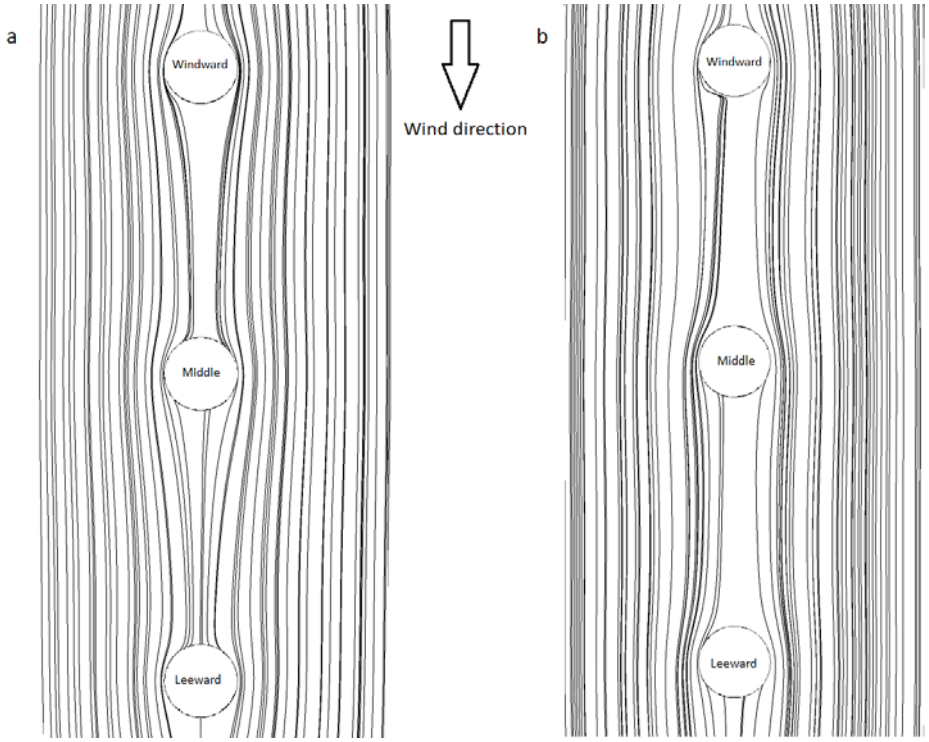

Figure 13. Surface velocity streamlines at height 5 m at a) v_{cw}=4 m/s b) v_{cw}=8 m/s at tower spacing 4.2D.

4.4. Conclusion

The influence of crosswind speed and tower spacing on the heat transfer performance of three NDDCTs arranged in line with respect to the prevailing wind direction has been studied. The flow and temperature fields were examined and the effect of tower spacing on each tower was discussed at various wind speeds. The overall heat transfer rate of the towers was found to be significantly different to that of the same tower placed alone. The windward tower acts like an isolated NDDCT at all crosswind speeds and tower-spacings except in a no-wind condition at a tower spacing of 1.8D. The windward tower protects the rear towers in most conditions. The interference of the towers at low wind speeds and tower-spacing results in a reduction of the middle-tower heat-transfer rate. By increasing the tower spacing, the protection provided by the windward tower from the upcoming wind decreases. Generally, an in-line arrangement of the towers can be applied in multi-tower systems

References

Cengel, Y.A., Ghajar, A.J., 2011. Heat and Mass Transfer: Fundamentals and Application. Heat and Mass Transfer Fundamental & Applications, 799-805.
Li, X., Duniam, S., Gurgenci, H., Guan, Z., Veeraragavan, A., 2017a. Full scale experimental study of a small natural draft dry cooling tower for concentrating solar thermal power plant. Applied Energy 193, 15-27.
Li, X., Guan, Z., Gurgenci, H., Lu, Y., He, S., 2015. Simulation of the UQ Gatton natural draft dry cooling tower. Applied Thermal Engineering.
Li, X., Guan, Z., Gurgenci, H., Lu, Y., He, S., 2016. Simulation of the UQ Gatton natural draft dry cooling tower. Applied Thermal Engineering 105, 1013-1020.
Li, X., Gurgenci, H., Guan, Z., Sun, Y., 2018. Experimental study of cold inflow effect on a small natural draft dry cooling tower. Applied Thermal Engineering 128, 762-771.

Li, X., Gurgenci, H., Guan, Z., Wang, X., Duniam, S., 2017b. Measurements of crosswind influence on a natural draft dry cooling tower for a solar thermal power plant. Applied Energy 206, 1169-1183.
Li, X., Xia, L., Gurgenci, H., Guan, Z., 2017c. Performance enhancement for the natural draft dry cooling tower under crosswind condition by optimizing the water distribution. International Journal of Heat and Mass Transfer 107, 271-280.
Lu, Y., Guan, Z., Gurgenci, H., Hooman, K., He, S., Bharathan, D., 2015. Experimental study of crosswind effects on the performance of small cylindrical natural draft dry cooling towers. Energy Conversion and Management 91, 238-248.
Lu, Y., Guan, Z., Gurgenci, H., Zou, Z., 2013. Windbreak walls reverse the negative effect of crosswind in short natural draft dry cooling towers into a performance enhancement. International Journal of Heat and Mass Transfer 63, 162-170.
Lu, Y., Gurgenci, H., Guan, Z., He, S., 2014. The influence of windbreak wall orientation on the cooling performance of small natural draft dry cooling towers. International Journal of Heat and Mass Transfer 79, 1059-1069.
Lu, Y., Klimenko, A., Russell, H., Dai, Y., Warner, J., Hooman, K., 2018. A conceptual study on air jet-induced swirling plume for performance improvement of natural draft cooling towers. Applied Energy 217, 496-508.
Wu, F.H.Y., Koh, R.C.Y., 1977. Mathematical Model for Multiple Cooling Tower Plumes. W. M. Keck Lab. of Hydraulics and Water Resources.
Wu, X.P., Yang, L.J., Du, X.Z., Yang, Y.P., 2014. Flow and heat transfer characteristics of indirect dry cooling system with horizontal heat exchanger A-frames at ambient winds. International Journal of Thermal Sciences 79, 161-175.
Yang, L.J., Du, X.Z., Yang, Y.P., 2011. Space characteristics of the thermal performance for air-cooled condensers at ambient winds. International Journal of Heat and Mass Transfer 54, 3109-3119.
Zhai, Z., Fu, S., 2006. Improving cooling efficiency of dry-cooling towers under cross-wind conditions by using wind-break methods. Applied Thermal Engineering 26, 1008-1017.
Zhao, Y., Sun, F., Li, Y., Long, G., Yang, Z., 2015. Numerical study on the cooling performance of natural draft dry cooling tower with vertical delta radiators under constant heat load. Applied Energy 149, 225-237.